Received: 7 August 2020 | Revised: 29 October 2020 | Accepted: 30 October 2020

DOI: 10.1002/jcc.26452



FULL PAPER

Journal of COMPUTATIONAL CHEMISTRY WILEY

# Prediction of lattice energy of benzene crystals: A robust theoretical approach

Anh L. P. Nguyen[1] | Thomas G. Mason[1] | Benny D. Freeman[2] | Ekaterina I. Izgorodina[1]

[1]School of Chemistry, Monash University, Clayton, Victoria, Australia

[2]Department of Chemical Engineering, The University of Texas at Austin, Austin, Texas, USA

**Correspondence**
Ekaterina I. Izgorodina, School of Chemistry, Monash University, 17 Rainforest Walk, Clayton, VIC 3800, Australia.
Email: katya.pas@monash.edu

## Abstract

We present an inexpensive and robust theoretical approach based on the fragment molecular orbital methodology and the spin-ratio scaled second-order Møller–Plesset perturbation theory to predict the lattice energy of benzene crystals within 2 kJ·mol$^{-1}$. Inspired by the Harrison method to estimate the Madelung constant, the proposed approach calculates the lattice energy as a sum of two- and three-body interaction energies between a reference molecule and the surrounding molecules arranged in a sphere. The lattice energy converges rapidly at a radius of 13 Å. Adding the corrections to account for a higher correlated level of theory and basis set superposition for the Hartree Fock (HF) level produced a lattice energy of −57.5 kJ·mol$^{-1}$ for the benzene crystal structure at 138 K. This estimate is within 1.6 kJ·mol$^{-1}$ off the best theoretical prediction of −55.9 kJ·mol$^{-1}$. We applied this approach to calculate lattice energies of the crystal structures of phase I and phase II—polymorphs of benzene—observed at a higher temperature of 295 K. The stability of these polymorphs was correctly predicted, with phase II being energetically preferred by 3.7 kJ·mol$^{-1}$ over phase I. The proposed approach gives a tremendous potential to predict stability of other molecular crystal polymorphs.

**KEYWORDS**

correlation, energy ab-initio, crystal structure, energy, gas-phase

## 1 | INTRODUCTION

By definition, polymorphs of a given molecule exist in different crystal structures, resulting in varying chemical and physical properties, undesired in many cases. Understanding structural and energetic factors leading to polymorphism in molecular crystals is crucial in directing the formation of a crystal with particular properties. New polymorphs have been known to emerge over time, thus suppressing the desirable properties of the material.[1–5] Experimental screening of all possible polymorphs is practically difficult, with the Food and Drug Administration guidelines suggesting a multitude of expensive characterization tests before a drug in crystalline form makes to the market.[6]

A substantial obstacle in studying polymorphs arises from the typically minuscule difference in their lattice energies under 4 kJ·mol$^{-1}$.[7–11] Thus, a theoretical method for predicting polymorphism must be able to properly capture the weak intermolecular interactions in molecular crystals.

Mostly used theoretical chemistry approach to predict lattice energies is density functional theory (DFT), whose accuracy is influenced by the choice of an exchange-correlation functional and inclusion of dispersion forces, e.g. through addition of the explicit empirical correction developed by Grimme—DFT-D3.[12] A study of the performance of the D3 correction with generalized gradient approximation (GGAs) and hybrid DFT functionals on the X23 data set[13–15] shows a mean absolute deviation (MAD) between 4.2 and 8.4 kJ·mol$^{-1}$ for the lattice energies of the 23 molecular crystals ranging from carbon dioxide to aspirin. This performance compares well with the available experimental results that were shown to also contain uncertainty

  

within 2.9 kJ·mol$^{-1}$.[16] Using the same database, the study of Reilly's et al.[17] investigated the performance of varying treatment of van der Waals (vdW; also referred to as dispersion) forces. In combination with the PBE0 functional, Tkatchenko–Scheffler (TS),[18] and many-body dispersion (MBD)[19–21] models gave MADs of 10.0 and 3.9 kJ·mol$^{-1}$, respectively. Despite its tremendous success, DFT-D3 falls short in predicting the correct order of polymorphs as reported in results of recent Blind Tests of organic structure prediction methods held by the Cambridge Crystallographic Data Centre.[22,23]

Second-order Möller–Plesset perturbation method, MP2, is an alternative to DFT as it is the cheapest among wavefunction-based methods to describe dispersion forces in molecular systems through explicit inclusion of electron correlation.[24–29] MP2 is not the most reliable method to choose as it is known to overestimate intermolecular interactions, especially of the $\pi$–$\pi$ stacking type.[30–33] Compared to DFT, MP2 still requires higher computational cost and hence its application has been limited to small- and medium-sized systems. MP2 in combination with a triple-$\zeta$ quality basis set on small molecular crystals such as ice XI, NH3, formic acid, HCN, CO2, and C2H2 showed a MAD of 3.1 kJ·mol$^{-1}$.[29] Del Ben et al. used a hybrid Gaussian and Plane waves (GPW) approach to significantly improve the scalability of the MP2 method. The resulting method in combination with Dunning's cc-pVTZ basis set produced a root mean squared deviation of 16.8 kJ·mol$^{-1}$ for lattice energies of 7 organic molecular crystals including benzene and uracil.[34]

The MP2 method is the cheapest post-Hartree-Fock method to treat correlation energy. However, it scales at O($N^5$), thus making its application to large-sized clusters of condensed systems impractical at present time. In order to facilitate these electronic structure calculations, the fragmentation approaches have been widely used to predict lattice energy of molecular crystals. The idea behind these fragmentation methods is to divide a large chemical system into small subsystems, for which quantum chemical calculations become computationally feasible. In his review in 2016,[35] Beran summarized three main schemes based on the fragmentation approach for studying molecular crystals: incremental methods,[36–39] hybrid many-body interaction,[40,41,42] and binary interaction.[41,43] In the incremental methods, only leading many-body terms (usually two- and three-body) are considered at a high level of theory, with higher-body terms being approximated with a lower level of theory. For example, HF can be used as the low level, while treating important many-body contributions at a correlated level such as MP2. This combination was applied to investigate the binding energy of ice $I_h$, giving an error of 1.9 kJ·mol$^{-1}$.[44] MP4 and CCSD(T) were also successfully used to treat many-body correlation effects and predict the lattice energy of rare gas crystals.[45] DFT functional has become popular to be used as a lower level of theory in the prediction of the lattice energies of benzene (PBE, an error of 7.7 kJ·mol$^{-1}$),[46] hexamine (PW91, an error of 9.6 kJ·mol$^{-1}$),[47] and urea (PW91, an error of 41.8 kJ·mol$^{-1}$).[47] The relative stability of the alpha and beta phases of diiodobenzene have been evaluated with the LDA, PBE, PBE0, and B3LYP functionals yielding values around −4.8 kJ·mol$^{-1}$, close to the quantum Monte Carlo result of −4.4 ± 3.6 kJ·mol$^{-1}$.[48] Instead of using electronic structure methods, the many-body terms can be evaluated with a force field, thus establishing what is now referred to as the hybrid many-body interaction (HMBI) approach. This approach used a classical force field to treat the long-range electrostatics and many-body induction effects to predict the lattice energy of seven molecular crystals (ice, formamide, acetamide, imidazole, benzene, $NH_3$, and $CO_2$) with errors of 2 to 4 kJ·mol$^{-1}$ compared to experiment.[49] The lattice energies of these molecular crystals were also predicted within the experimental values using the polarizable force field that involves the distributed multiple moments, distributed polarisabilities and two- and three-body atomic dispersion coefficients.[50] The HMBI method that incorporates the ab initio molecular dynamic simulations to describe the intermolecular electrostatics, induction, two- and three-body dispersion has been also employed for studying the energetic stability of polymorphs of aspirin,[51] oxalyl dihydrazide,[52] and ice XV.[53] Contrary to the incremental and hybrid many-body interaction methods, the binary interaction method considers one- and two-body terms while neglecting higher-body terms. The significant difference of this method to the other two is that fragments, of the one- and two-body types, are embedded in the electrostatic environment of point charges and dipoles of the molecular system itself. The binary interaction method was developed by Hirata and co-workers and applied to the crystal structures of formic acid, which predicted the correct stabilities of its polymorphs.[41] Moreover, this method has been successfully employed to investigate the properties of many molecular crystals such as hydrogen fluoride,[54] ice,[55] and carbon dioxide.[56] This method is a simplification of the fragmenting molecular orbital (FMO) model.[57–59] Another embedding method introduced by Manby[60] includes exchange-repulsion in addition to the electrostatic field, which has successfully predicted crystal energies for carbon dioxide (an error of 2.6 kJ·mol$^{-1}$ from experiment),[60] ice polymorphs (an error of 2.1 kJ·mol$^{-1}$ from experiment),[60,61] hydrogen fluoride (an error of −1.1 kJ·mol$^{-1}$ of the theoretical value calculated with MP2/aug-cc-pVTZ[54]),[60] and clathrate hydrates (an error 4.2 kJ·mol$^{-1}$ from the quantum Monte Carlo benchmark value).[62] Recently, He and co-workers applied the electrostatically embedded generalized molecular fractionation with conjugate caps (EE-GMFCC)[63,64] on the large clusters of ions and waters that produced the accurate electronic energies within 30 kJ·mol$^{-1}$ of the full quantum mechanical calculations.[63] Despite the advances made in the prediction of lattice energies of molecular crystals, the currently available methods still require significant computational resources to afford these calculations.

To achieve results comparable with experiment, these electronic structure methods are usually applied along with periodic boundary conditions (PBCs). The role of PBCs is to replicate the unit cell in space to create a large supercell, thus emulating the bulk.[65] Despite its wide application in condensed matters, the PBC approach has several limitations. A distance cut-off, which must be shorter than half the length of the unit cell, is implemented to avoid molecules in the simulation box interacting with themselves. This truncation causes discontinuity in the potential function and its derivatives. Equally important, a tail correction must be introduced to account for missing contributions to the total energy as a result of the potential

truncation. Since the tail correction cannot be accurately calculated for the simulation box, long range electrostatics, a crucial ingredient of the bulk phase intermolecular interactions, is usually described with an approximation such as the Ewald summation.[66] This method accelerates the convergence of the sum of the Coulombic energies over the whole simulation box by splitting it into two exponentially converging sums.[67]

Yang et al.[68] recalculated the experimental sublimation enthalpy of the crystalline benzene structure at 138 K by introducing a thermal correction and a zero point energy (ZPE), producing the lattice energy of −55.3 ± 2.2 kJ·mol$^{-1}$. For the theoretical approach, they implemented a fragmentation scheme to split the system into a series of two-, three- and four-body interactions, or the so-called dimers, trimers, and tetramers, respectively. The HF energies were determined by summing up all many-body terms (14 dimers, 8 trimers, and 8 tetramers) under the PBCs. The dispersion part of each many-body contribution (50 dimers, 96 trimers, and 8 tetramers) was calculated with the best (in terms of accuracy) quantum chemical method available to-date—OSV-CCSD(T0)-F12, an orbital-specific-virtual, explicitly correlated, local coupled cluster method with perturbative triples. For long-range interactions, 8737 dimers and 312,855 trimers were summed over. The predicted lattice energy was found to be −54.58 ± 0.76 kJ·mol$^{-1}$. After accounting for the relaxation energy of −1.32 ± 0.1 kJ·mol$^{-1}$ required for the benzene crystal to undergo the transition from 138 to 0 K, the best predicted lattice energy benzene was found to be −55.90 ± 0.76 kJ·mol$^{-1}$.

Recently Sherrill and co-workers[69] have also employed the fragmentation method to calculate the lattice energy of the 138 K crystalline benzene structure with the HF-3c[70] method. As HF-3c does not capture the three-body dispersion, the Axilrod–Teller–Muto (ATM) potential was also added to rectify the situation, yielding the lattice energy of −57.60 kJ·mol$^{-1}$. Their algorithm made a replica of the unit cell of the 138 K structures seven times along each coordinate directions, reproducing a large enough supercell that could fit a crystalline sphere of a radius equivalent to a given value of 15 Å. They used a slightly different definition of the lattice energy by calculating many-body contributions with respect to a reference molecule placed nearest to the center of the supercell. The resulting lattice energy included two- and three-body contributions. This approach is similar to the direct summation calculation of the Madelung constant of a crystal structure[71] using the Harrison approach[72] of expanding spheres surrounding the molecule at the origin.[73]

In both of these papers the fragmentation scheme did not contain an embedding potential, thus requiring the inclusion of up to four-body contributions in the study of Yang et al.[68] to predict the most accurate lattice energy of the benzene crystal to-date. Our group has recently introduced a modified version of MP2, the spin-ratio scaled second-order Møller-Plesset perturbation method (SRS-MP2)[74,75] that predicts intermolecular interactions within chemical accuracy (2 kJ·mol$^{-1}$ on average) with a relatively small basis set, Dunning's cc-pVTZ basis set, and without the need to account for the basis set superposition error for electron correlation. The excellent performance of SRS-MP2 stems from the scaling of both opposite-spin (OS) and same-spin (SS) components in the MP2 correlation energy to reproduce benchmark interaction energies of both neutral and ionic intermolecular complexes present in the S22,[76] S66,[77] and IL174[78,79] databases.

$$E_{Corr}^{MP2} = c_{OS} * E_{OS}^{MP2} + c_{SS} * E_{SS}^{MP2} \quad (1)$$

The OS and SS coefficients depend on the ratio of OS to SS interaction energy and must be independently fitted for each basis set. Even though the conventional MP2 method does not capture the three-body dispersion effect,[80,81] its modification, the SRS-MP2 method, incorporates this effect through the opposite- and same-spin coefficients that were fitted to reproduce interaction energies of CCSD(T)/CBS, the "gold standard" method in ab initio theory. The SRS-MP2 approach has been shown to produce similar accuracy as the benchmark method of coupled-cluster theory, CCSD(T), when applied within the complete basis set.

Fragment molecular orbital (FMO) approach enables quantum chemical calculations of condensed systems through dividing them into fragments, with two- and three-body interactions being calculated individually.[82–84] This division leads to a high level of parallelism on modern supercomputers. Unlike the binary methods, in the FMO method, higher many-body terms such as three-body are included in the calculations. It should be noted that all one-, two-, and three-body terms are treated at the same level of quantum chemical theory. In molecular crystals, single molecules can be regarded as fragments without breaking any chemical bonds. The total energy of the system is calculated by summing up energies of single molecules (denoted as FMO1) as well as two-(denoted as FMO2) and three-body (denoted as FMO3) contributions. In the FMO approach, individual fragments are placed in an electrostatic potential field (ESP) or a Coulomb bath that is generated by the electric field of all the molecules in the system. This ensures that the polarization effects are indirectly included in two- and three-body calculations. Since the FMO approach incorporates the polarization environment through the Coulomb bath, it is unnecessary to consider many-body effects beyond three-body contributions. The calculation cost can be further reduced through neglecting some of the two- and three-body interactions. Inclusion of these cut-offs can compromise the accuracy of resulting energies.[85–90] Recently, our group published an extensive study on the effect of many-body cut-offs in large-scale clusters of ionic liquids (consisting of up to 64 ions) to ensure spectroscopic accuracy of both HF and correlation many-body contributions to electronic energies.[91]

This work was inspired by the Harrison method that we previously applied to calculating Madelung constants of inorganic and organic ionic salts.[71] A spherical approach was applied to predict lattice energy of the available benzene crystal structures in combination with the FMO approach and the SRS-MP2 method. A reference molecule was randomly selected near the center of the unit cell prior to the calculation. The well-studied 138 K crystal structure of benzene (code BENZEN01 in the Cambridge Structural Database),[92] as well as two recently identified polymorphs of benzene[93]—labeled phase I and phase II—were considered. Phase I is orthorhombic with a space group

*Pbca*, while phase II crystallizes in a monoclinic structure of a space group $P2_1/c$.[93]

Phase I and the benzene crystal structure at 138 K[92] are isomorphic, except for the elongation of the lattice parameters due to the thermal effect. Phase II differentiates from phase I in the orientation of the CH$\cdots\pi$ interactions. In phase I, two benzene molecules responsible for such interaction are almost perpendicular, confining an empty spaces or void with their neighboring molecules.

Due to the inclusion of indirect polarization effects at the monomer level, the lattice energy converged rapidly with increasing radius of the sphere, producing accurate results with a radius of 13 Å in all three crystal structures. Two additional corrections were introduced to improve the accuracy of lattice energy—a counterpoise correction at the HF level to account for basis set superposition error and a correction for higher correlated level of theory calculated with CCSD(T) for dimers and trimers with immediate contact with the reference molecule. The thus calculated lattice energy of −57.5 kJ·mol$^{-1}$ for the 138 K benzene crystal structure was only 1.6 kJ·mol$^{-1}$ higher than the best theoretical result of Yang et al.[68] The instantaneous analysis of energetic components of lattice energy revealed that the HF

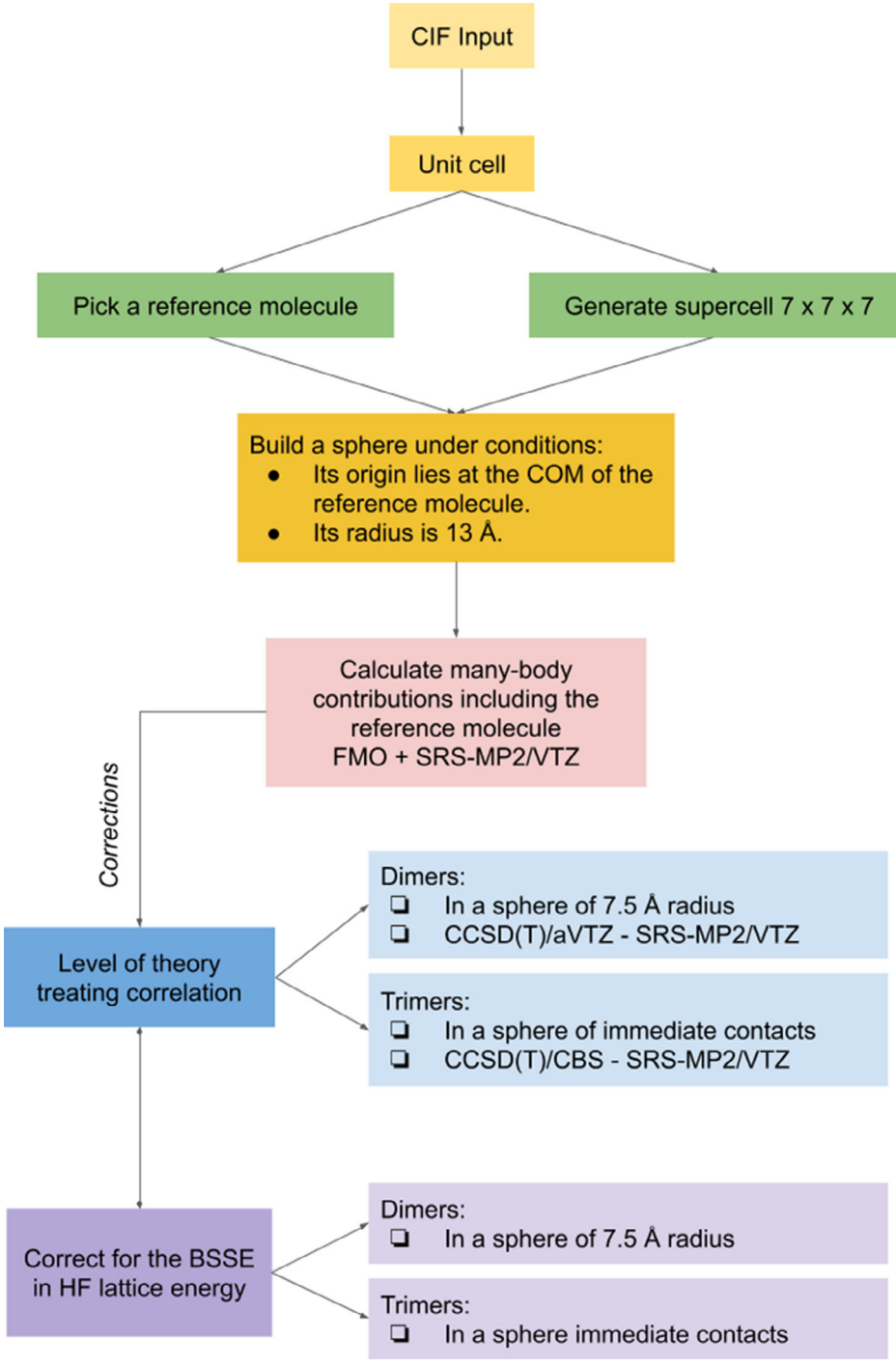


**FIGURE 1** Flowchart of calculating the lattice energy [Color figure can be viewed at wileyonlinelibrary.com]

(i.e., electrostatic) component was rather positive above 12.4 kJ·mol$^{-1}$ and the structure was driven by a strong dispersion (i.e. electron correlation) component of −85.7 kJ·mol$^{-1}$. Within the FMO approach, three-body contributions were found to be below chemical accuracy. Lattice energies of phase I and phase II were calculated to be −46.6 and −50.3 kJ·mol$^{-1}$, respectively. Phase II was found to be more thermodynamically stable which is in good agreement with experiment. Phase I and II were found to be predominantly stabilized with dispersion forces. Whereas the electrostatic component in phase II was found to be strongly repulsive on the scale of 16.6 kJ·mol$^{-1}$, it was calculated to be only 1.5 kJ·mol$^{-1}$ in phase I, clearly identifying a different energetic landscape of the two phases. The proposed approach has demonstrated its accuracy for the prediction of lattice energy of benzene and offers straightforward strategy for studying energetics of other organic molecular crystals and their polymorphs. The advantage of using the FMO approach also allows for an instantaneous analysis of two- and three-body contributions as well as electrostatic and dispersion components of lattice energy, thus giving invaluable insight into the energetic landscape of these polymorphs and developing strategies to discourage the formation of multiple polymorphs.

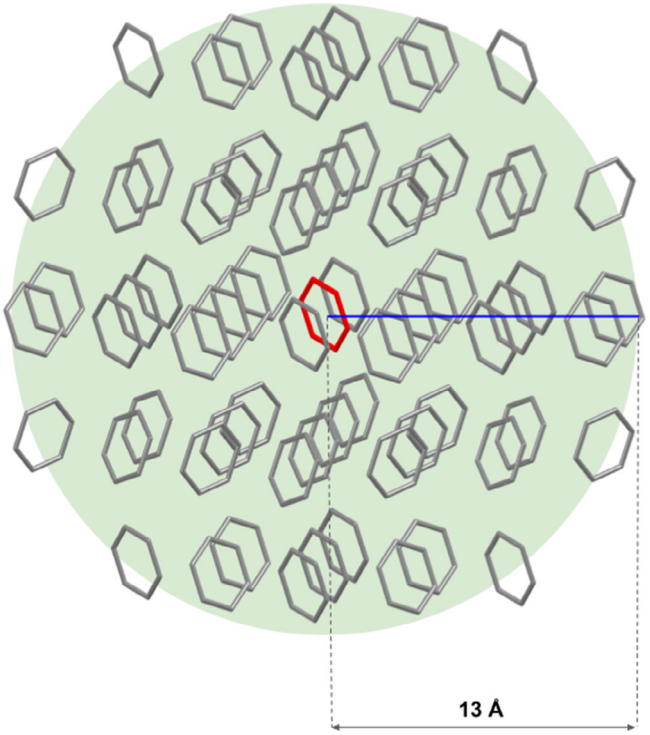


**FIGURE 2** A crystalline sphere around the reference molecule (in red) with a radius of 13 Å [Color figure can be viewed at wileyonlinelibrary.com]

## 2 | METHODOLOGY

The complete protocol for the calculation of lattice energy is summarized in Figure 1. For each benzene crystal structure, an arbitrary benzene molecule is chosen as the reference molecule and is placed in the center of a sphere with a radius of 13 Å. In order to create this sphere, a distance between the centers of mass (COMs) of the reference molecule and other neighboring molecules were compared to this radius to determine whether the molecule should remain in the sphere, see Figure 2.

All FMO calculations were performed with the GAMESS-US software package.[94] The SRS-MP2/cc-pVTZ method[74] was then used to perform a single point calculation on the sphere. For this basis set, the opposite-spin coefficient of 1.64 was used, whereas the same-spin coefficient was set to zero as the spin ratio was found to be >1.0 in benzene dimers. The Mulliken atomic population scheme and the Mulliken point charge scheme implemented to approximate the Coulomb bath were disabled by setting RESPAP to 0 and RESPPC to −1, respectively, as demonstrated previously to reduce large errors in electronic energy.[91] No truncations were used for two- and three-body contributions for both HF and SRS-MP2 levels of theory. Only the interaction energies between the reference molecule and other molecules in the sphere were considered in the calculation of lattice energies ($E^{latt}$) as shown below:

$$\begin{aligned} E^{latt} = {} & E_{Ref}^{FMO1} - E_{Ref}^{Vac} \\ & + E_{SRSMP2}^{\Delta FMO2} + E_{HF}^{\Delta FMO2} + E_{ESP}^{\Delta FMO2} \\ & + E_{SRSMP2}^{\Delta FMO3} + E_{HF}^{\Delta FMO3} + E_{ESP}^{\Delta FMO3} \\ & + \Delta CCSD(T) + BSSE_{HF} \end{aligned} \tag{2}$$

where $E_{Ref}^{FMO1}$ is FMO1 energy of the reference molecule, $E_{Ref}^{Vac}$ is the energy of the reference molecule in a vacuum calculated with SRS-MP2/cc-pVTZ, $\Delta FMO2$ terms represent two-body energies, further separated into the HF, correlation (SRS-MP2), and electrostatic potential (ESP) contributions, $\Delta FMO3$ terms represent three-body energies, $\Delta CCSD(T)$ is the correction for a higher correlated level of theory, and $BSSE_{HF}$ is counterpoise correction for HF.

Although rather elegant, the approach puts a strong emphasis on the accuracy of the underlying quantum chemical method used. In order to achieve the spectroscopic (i.e., sub KJ · mol$^{-1}$ accuracy), the SRS-MP2 energies of the close-contact two- and three-body interactions with the reference molecule were corrected to the golden standard method, CCSD(T). For two-body contributions, the monomers, whose centers of mass lie within the sphere of 7.5 Å, are considered as close contacts to the reference molecule. For three-body contributions, the close contacts were defined as those located in the first molecular solvation around the reference molecule. Even though the differences between SRS-MP2 and CCSD(T) energies are relatively small in value (below 1 kJ·mol$^{-1}$), the sheer number of close contact interactions (between −0.2 and 0.8 kJ·mol$^{-1}$) leads to error accumulation. For two-body interactions, the CCSD(T)/aug-cc-pVTZ method was used, whereas for three-body interactions were calculated with CCSD(T) within the complete basis set (CBS) using the following Formula (3):

$$\begin{aligned} CCSD(T)/CBS = {} & \Delta CCSD(T)/aDZ \\ & + \frac{MP2/aQZ * 4^3 - MP2/aTZ * 3^3}{4^3 - 3^3} \end{aligned} \tag{3}$$

*aDZ* , *aTZ*, and *aQZ* in Equation (3) represent aug-cc-pVDZ, aug-cc-pVTZ, and aug-cc-pVQZ basis sets, respectively. One of the

advantages of the SRS-MP2 method is the inclusion of the BSSE in the fitted coefficients of correlation energy. However, the HF component of the total SRS-MP2 energy still suffers from BSSE. The HF energies of two-body interactions were corrected using the conventional approach of Boys and Bernardi.[95] For three-body interactions among molecules I, J and K, abbreviated as *3B-INT*, the counterpoise correction was calculated using the following equation:

$$\Delta E_{IJK}^{3B-INT} = E_{IJK}^{\chi_{IJK}} - E_{IJ}^{\chi_{IJK}} - E_{IK}^{\chi_{IJK}} - E_{JK}^{\chi_{IJK}} + E_{I}^{\chi_{IJK}} + E_{J}^{\chi_{IJK}} + E_{K}^{\chi_{IJK}} \quad (4)$$

The one- and two-body energies were calculated within the basis sets of the I, J, and K molecules, $\chi_{IJK}$. It has to be noted that when conventional counterpoise correction between two interacting molecules cannot be negative, the counterpoise correction for three interacting molecules can be either positive or negative. The calculations for

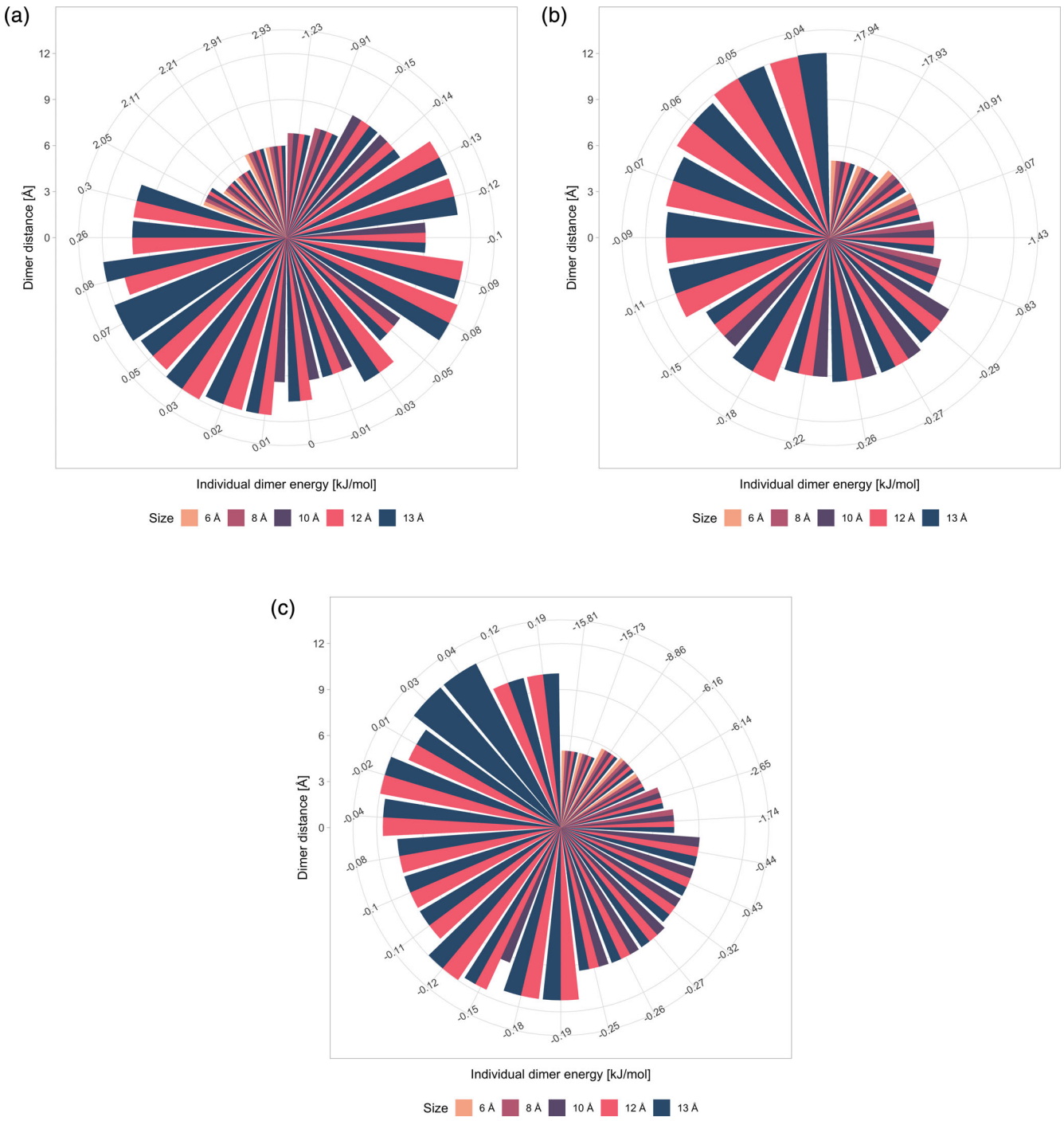


**FIGURE 3** Individual two-body contributions in spheres of varying size: (a) HF energy, (b) correlation energy, (c) Total contribution [Color figure can be viewed at wileyonlinelibrary.com]

correcting the correlated level of theory and for counterpoise corrections were performed with Psi4 software.[96]

## 3 | RESULTS AND DISCUSSIONS

### 3.1 | Benzene structure at 138 K

Individual energies of the two- and three-body contributions with respect to the distance to the reference molecule (as shown in Equation (2)) are presented in Figures 4 and 5, respectively. As already mentioned above, we only account for dimers and trimers due to the use of the FMO approach. For three-body contributions, the shorter of two distances was taken.

The two- and three-body energies can be further split into the HF and correlation energies, which are shown on the first and second diagrams of each figure (see Table S1). The sum of both energy terms gives the total contributions that are displayed on the third diagrams. Different colors on Figures 3 and 4 indicate different sizes of the crystalline sphere ranging from 6 to 13 Å. The length of the bars

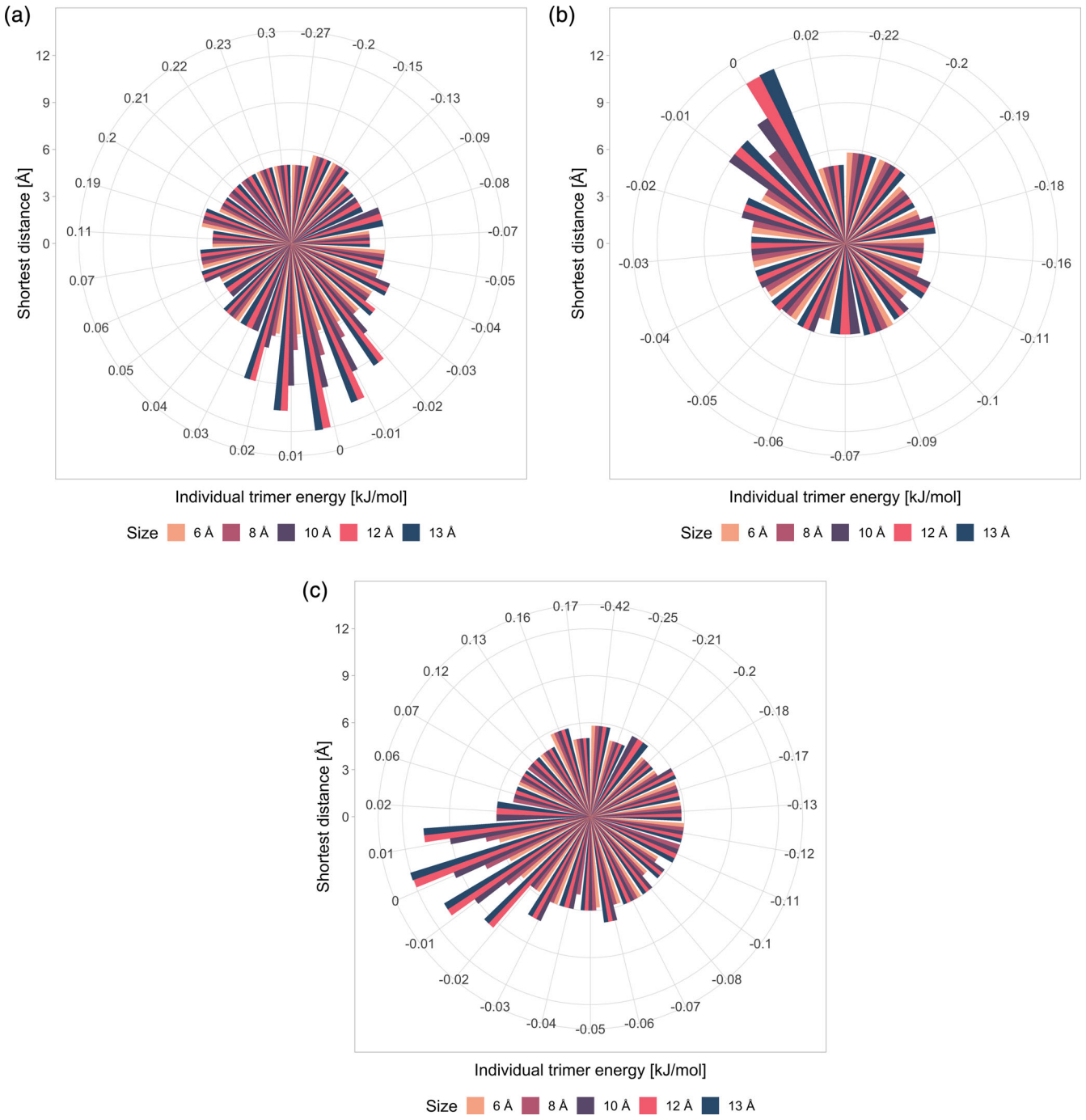


**FIGURE 4** Individual three-body contributions in spheres of varying size: (a) HF energy, (b) correlation energy, (c) Total contribution [Color figure can be viewed at wileyonlinelibrary.com]

| Sphere | $E_{SRSMP2}^{\Delta FMO2}$ | $E_{HF}^{\Delta FMO2}$ | $E_{Corr}^{\Delta FMO2}$ | $E_{ESP}^{\Delta FMO2}$ | $E_{SRSMP2}^{\Delta FMO3}$ | $E_{HF}^{\Delta FMO3}$ | $E_{Corr}^{\Delta FMO3}$ | $E_{ESP}^{\Delta FMO3}$ |
|---|---|---|---|---|---|---|---|---|
| 6 Å | −47.3 | 9.3 | −55.9 | −0.7 | −0.5 | 0.2 | −0.8 | 0.1 |
| 8 Å | −66.8 | 12.1 | −78.1 | −0.9 | −1.7 | 0.6 | −2.5 | 0.3 |
| 10 Å | −69.5 | 11.7 | −80.3 | −0.9 | −2.7 | 0.7 | −3.8 | 0.4 |
| 12 Å | −70.2 | 12.1 | −81.4 | −0.9 | −3.0 | 0.5 | −4.2 | 0.7 |
| 13 Å | −70.2 | 12.2 | −81.5 | −0.9 | −3.0 | 0.4 | −4.2 | 0.7 |

**TABLE 1** Components of FMO lattice energy of benzene crystal structure at 138 K

demonstrates the distance in dimers and the shorter distance in trimers. The indexes on the circle show the values of contributing energies.

Generally, dimers with distances between monomers below 8 Å contribute significantly to the lattice energy. These dimers also have large and positive electrostatic energy, whereas for dimers with distances longer than 10 Å electrostatic contributions are negligible, below 0.3 kJ·mol$^{-1}$, with majority of these being even slightly negative of −0.1 kJ·mol$^{-1}$ on average. Not surprisingly, the two-body dispersion contributions are almost always attractive falling in the range of −0.02 and −15.8 kJ·mol$^{-1}$ with increasing distance between monomers. Overall, the total two-body dispersion of −81.5 kJ·mol$^{-1}$ dominates the final lattice energy, whereas two-body electrostatics destabilizes the crystal structure by as much as 12.2 kJ·mol$^{-1}$.

In comparison to two-body contributions, individual three-body interaction energies vary insignificantly. Even trimers with the contact below 6 Å demonstrate small contributions below an absolute value of 0.5 kJ·mol$^{-1}$. Trimers with the distance above 9 Å contribute close to 0.0 kJ·mol$^{-1}$. Some three-body dispersion energies are positive, whereas the majority of these contributors are attractive up to −0.22 kJ·mol$^{-1}$. Individual three-body electrostatic energies also fall in a very narrow range from −0.3 to 0.3 kJ·mol$^{-1}$, making the total three-body contribution of −3.0 kJ·mol$^{-1}$ to the lattice energy practically negligible.

Due to the nature of FMO calculations, the sphere with a radius of 13 Å can be split into smaller-sized spheres with radii of 6, 8, 10, or 12 Å. The sum of individual two- and three-body contributions, together with their electrostatic (HF) and dispersion (correlation energy calculated at SRS-MP2) components, incorporated into each sphere size are given in Table 1.

Analysis of these contributions depicts a relatively fast convergence of both two- and three-body effects with increasing sphere radius. Already the 10 Å sphere produces the lattice energy that deviates only by 1.2 kJ·mol$^{-1}$ from that of the 13 Å sphere. Overall, the electrostatic forces show a repulsive effect, with the benzene molecules being strongly stabilized through dispersion energy. The fast convergence is attributed to additional polarization effects accounted for in the FMO approach through the Coulomb bath compromised of the electron density of all monomers. It has to be noted that the contribution from the Coulomb bath appears to have converged already with the 12 Å sphere. The two-body contributions constitute 96% of the resulting lattice energy, whereas the three-body contributions are as little as 4%.

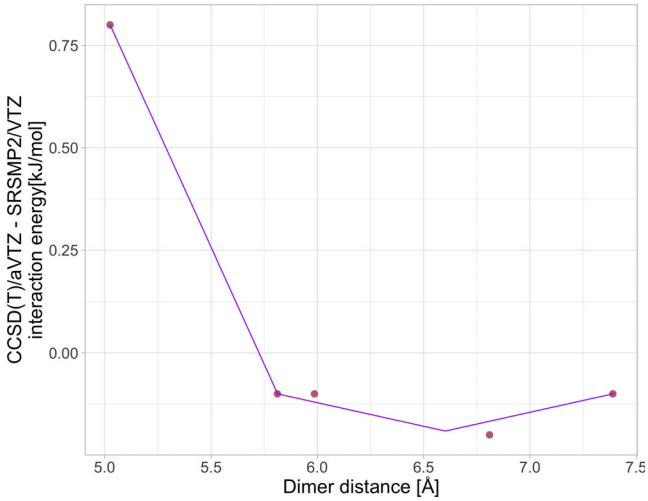


**FIGURE 5** Difference between two-body CCSD(T)/aug-cc-pVTZ and SRS-MP2/cc-pVTZ correlation interaction energy with respect to distance to the reference molecule [Color figure can be viewed at wileyonlinelibrary.com]

The lattice energy comprised of the sum of the two- and three-body contributions with respect to the reference molecule is calculated to be −73.2 kJ·mol$^{-1}$. According to Equation (2), this number must be corrected for the difference between the energy of the reference molecule in the Coulomb bath and in vacuum, which in the case of the benzene crystal structure at 138 K is found to be 9.3 kJ·mol$^{-1}$, thus making the lattice energy of a value of −63.9 kJ·mol$^{-1}$.

The correlation interaction energy calculated with SRS-MP2 is still not as accurate as the "golden standard" method, the coupled-cluster method with singles and doubles and noniterative triples (CCSD(T)). This only affects contributions from molecules located within the close contact, 7.5 Å, to the reference molecule as demonstrated before on the potential energy surfaces of the S66 database.[75] Figure 5 shows the difference in two-body correlation interaction energies between CCSD(T)/aug-cc-pVTZ and SRS-MP2/cc-pVTZ.

A similar trend between SRS-MP2 and CCSD(T) correlation interaction energies is found for benzene dimers with increasing intermolecular distance. Individual differences are always below 1.0 kJ·mol$^{-1}$ (see Table S2) and their convergence is observed at around 7 Å. The correction for the CCSD(T) level of theory for two-body contributions delivers as little as 0.6 kJ·mol$^{-1}$, which is an excellent outcome. Figure 6 reveals the structures of benzene dimers that

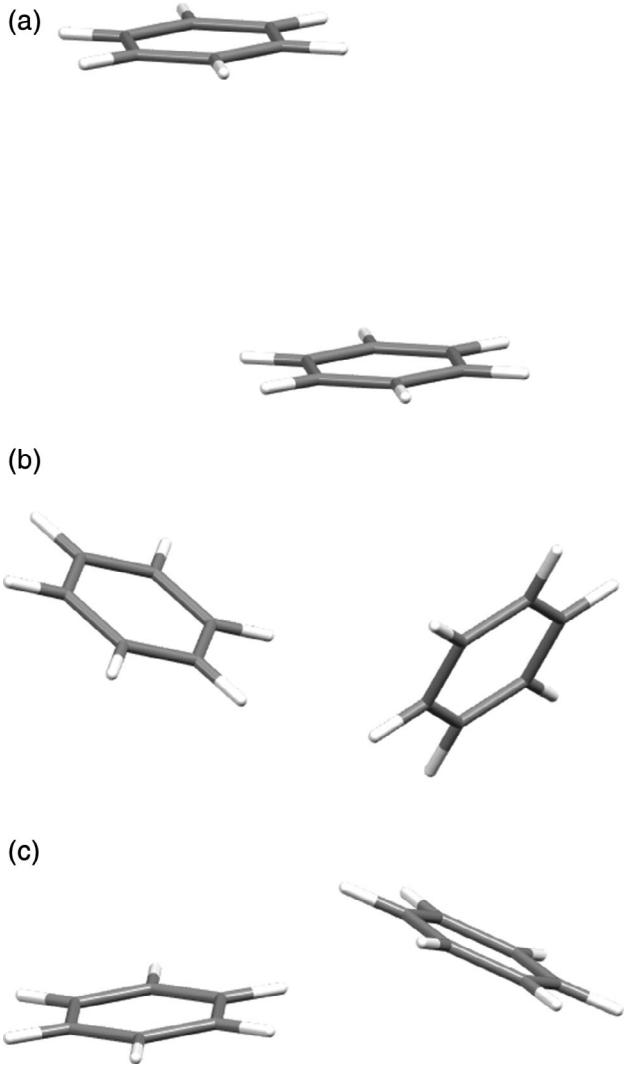


**FIGURE 6** Typical structures of benzene dimers being overestimated of SRS-MP2

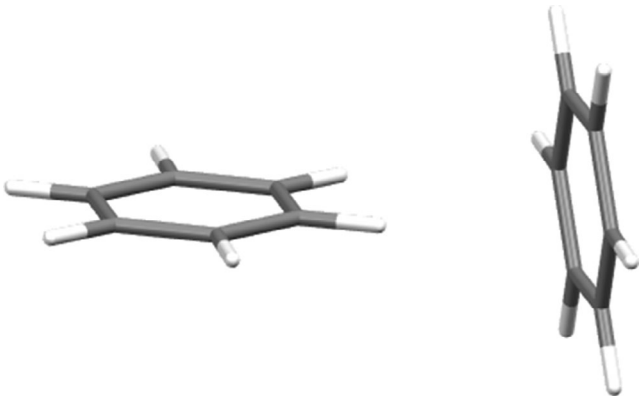

**FIGURE 7** T-shaped dimers being underestimated by SRS-MP2

are slightly underestimated by the SRS-MP2 method within 0.25 kJ·mol$^{-1}$. These dimers exhibit parallel displaced, V-shaped, and tilted geometries. In the case of the T-shaped dimers, shown in

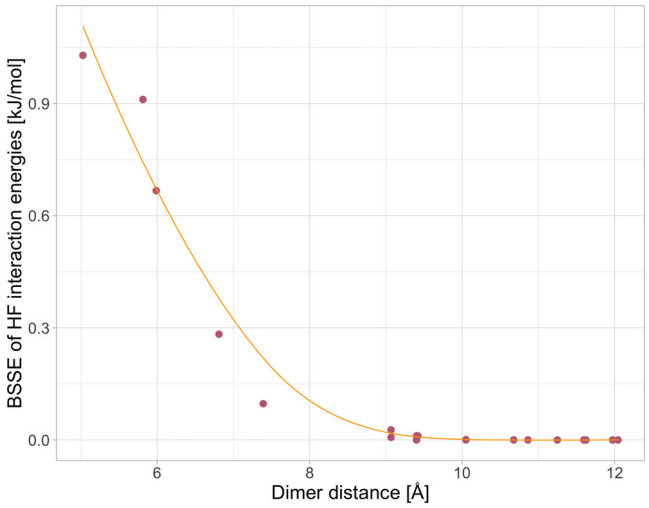


**FIGURE 8** Individual BSSE corrections for two-body contributions at the HF level of theory [Color figure can be viewed at wileyonlinelibrary.com]

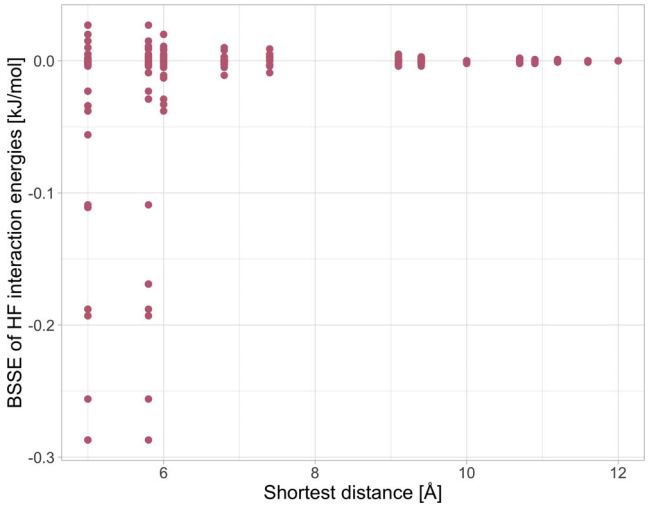


**FIGURE 9** Individual BSSE corrections for three-body contributions at the HF level of theory [Color figure can be viewed at wileyonlinelibrary.com]

Figure 7 the SRS-MP2 method overestimates the correlation energy by 0.8 kJ·mol$^{-1}$, the largest deviation observed.

Since the SRS-MP2 method deviation for two-body effects was found to be rather small vanishing at longer distances, among three-body contributions only those in the immediate contact with the reference molecule were corrected with CCSD(T)/CBS (for more detail see Theoretical procedures). In general, the SRS-MP2 method overestimated these contributions in the range of 0.3 kJ·mol$^{-1}$ (see Table S3), with the correction for the higher level of theory being calculated as little as 0.4 kJ·mol$^{-1}$.

In order to further improve the accuracy of the predicted lattice energy, a correction for basis set superposition error at the HF level must be introduced. Individual corrections for two- and three-body

**TABLE 2** Components of FMO lattice energy of phase I

| Sphere | $E_{SRSMP2}^{\Delta FMO2}$ | $E_{HF}^{\Delta FMO2}$ | $E_{Corr}^{\Delta FMO2}$ | $E_{ESP}^{\Delta FMO2}$ | $E_{SRSMP2}^{\Delta FMO3}$ | $E_{HF}^{\Delta FMO3}$ | $E_{Corr}^{\Delta FMO3}$ | $E_{ESP}^{\Delta FMO3}$ |
|---|---|---|---|---|---|---|---|---|
| 6 Å | −43.7 | −0.3 | −43.1 | −0.4 | −0.2 | 0.6 | −0.8 | 0.0 |
| 8 Å | −58.2 | 0.2 | −57.8 | −0.6 | −0.8 | 2.0 | −2.4 | −0.4 |
| 10 Å | −60.1 | −0.1 | −59.4 | −0.6 | −1.4 | 2.0 | −3.2 | −0.3 |
| 12 Å | −60.7 | 0.2 | −60.3 | −0.6 | −1.7 | 1.6 | −3.5 | 0.2 |
| 13 Å | −60.7 | 0.3 | −60.4 | −0.6 | −1.7 | 1.5 | −3.5 | 0.3 |

**TABLE 3** Components of FMO lattice energy of phase II

| Sphere | $E_{SRSMP2}^{\Delta FMO2}$ | $E_{HF}^{\Delta FMO2}$ | $E_{Corr}^{\Delta FMO2}$ | $E_{ESP}^{\Delta FMO2}$ | $E_{SRSMP2}^{\Delta FMO3}$ | $E_{HF}^{\Delta FMO3}$ | $E_{Corr}^{\Delta FMO3}$ | $E_{ESP}^{\Delta FMO3}$ |
|---|---|---|---|---|---|---|---|---|
| 6 Å | −49.3 | 11.1 | −59.8 | −0.6 | −1.1 | 0.3 | −1.5 | 0.0 |
| 8 Å | −63.8 | 15.0 | −77.9 | −0.8 | −1.6 | 2.4 | −3.5 | −0.5 |
| 10 Å | −65.3 | 15.6 | −79.9 | −1.0 | −2.7 | 2.0 | −4.9 | 0.2 |
| 12 Å | −66.2 | 15.4 | −80.6 | −1.0 | −3.0 | 2.0 | −5.2 | 0.2 |
| 13 Å | −66.5 | 15.4 | −80.9 | −1.0 | −3.1 | 2.0 | −5.3 | 0.2 |

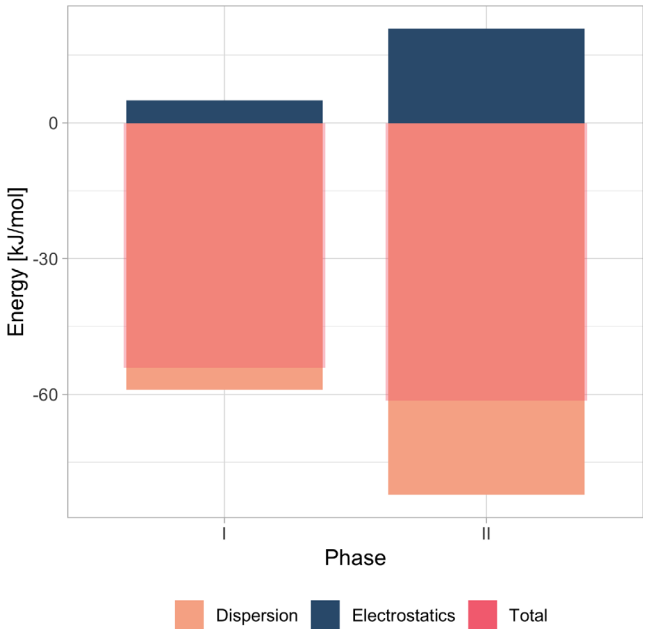


**FIGURE 10** Components of lattice energy of phases I and II [Color figure can be viewed at wileyonlinelibrary.com]

contributions (see Tables S4 and S5) with increasing distance between monomers are presented in Figures 8 and 9, respectively. Analysis of these data reveals that BSSE starts to diminish at a short distance of 8 Å, highlighting the local nature of the effect. The BSSE corrections for two- and three-body HF interaction energies were calculated to be 5.5 and −0.11 kJ·mol$^{-1}$, respectively.

The inclusion of both corrections accounting for a higher correlated level of theory and BSSE gives a new predicted value of −57.5 kJ·mol$^{-1}$ of the benzene crystal structure at 138 K. This result is within 1.6 kJ·mol$^{-1}$ of the value of −55.9 kJ·mol$^{-1}$ reported by Yang et al.[68] and within 1.2 kJ·mol$^{-1}$ of the value of −56.3 kJ·mol$^{-1}$ reported by Sherrill et al.[69]

## 3.2 | Benzene polymorphs at 295 K

The approach proposed in this work was assessed for two polymorphs of benzene reported at 295 K known as phase I and phase II. Following the procedure in the flowchart 1 for calculating the lattice energy, spheres of the 13 Å radius were created for the crystal structures of phase I and II with an arbitrary reference molecule at the center. Lattice energy results from the FMO3 + SRS-MP2/cc-pVTZ calculations are displayed in Tables 2 and 3 for phase I and II, respectively.

Like the crystal structure at 138 K, phase I also shows a fast convergence with the increasing sphere size, with a radius of 12 Å being sufficient to predict lattice energy. For phase I, the two-body electrostatic contributions of as little as 0.3 kJ·mol$^{-1}$ to lattice energy is practically negligible. Three-body electrostatic contributions are repulsive of 1.5 kJ·mol$^{-1}$ in magnitude. The dispersion forces predominantly contribute to lattice energy, with both two-body contributions playing an important role (see Table S6). Overall, the three-body effect is rather negligible due to the cancellation of electrostatic and dispersion forces. The electrostatics contributes 3% of the absolute value of the dispersion energy (see Figure 10). The lattice energy of phase I prior to corrections was calculated to be −54.1 kJ·mol$^{-1}$.

Similar to other phases, the lattice energy of phase II converges even faster with a radius of 10 Å. The difference to phase I lies in the strong repulsive nature of electrostatic forces contributing up to 17.4 kJ·mol$^{-1}$. The dispersion force was again found to predominantly contribute to the final lattice energy. The ratio of electrostatics to the absolute value of the dispersion energy is 20%, higher than in phase I (see Figure 10). The two-body effects play by far a more important role in the cohesion of this phase, with three-body effects being small but non-negligible. Without additional corrections, phase II was calculated to have a lattice energy of −61.5 kJ·mol$^{-1}$ (see Table S11).

To this end, it can be concluded that phase II is energetically more stable than phase I, which is in agreement with experimental observations. Previous theoretical calculations identified that phase II was thermodynamically more stable at higher pressures compared to

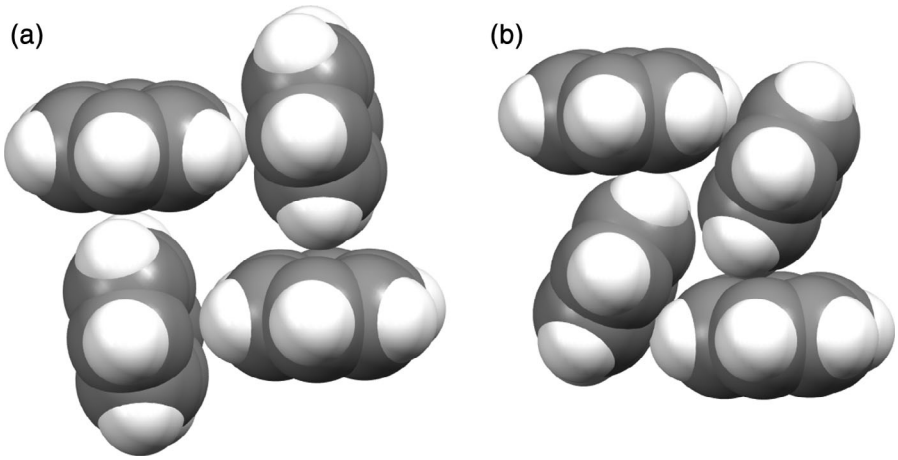


**FIGURE 11** Molecular arrangements in two polymorphs

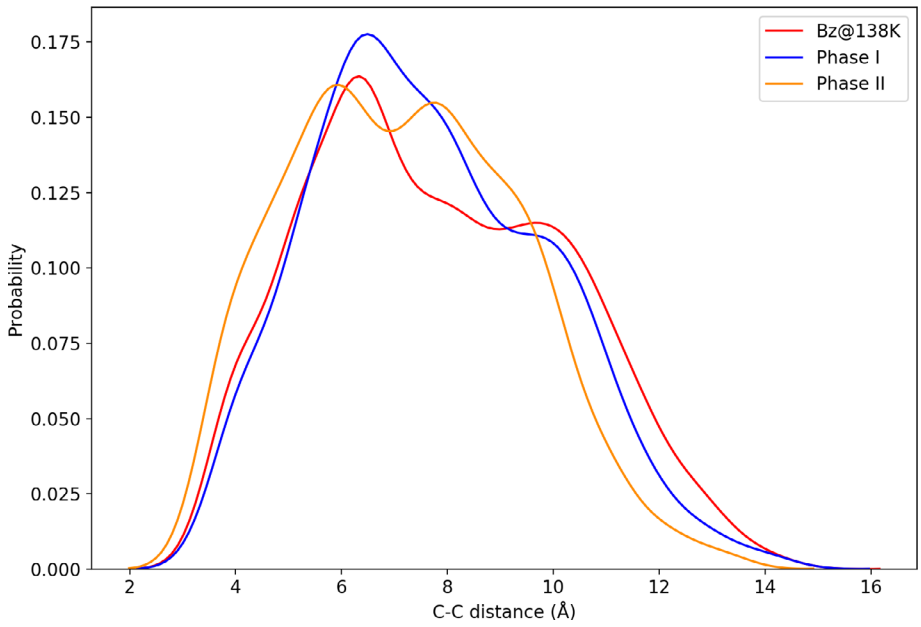


**FIGURE 12** Distribution of the C—C intermolecular distances of the benzene crystal structures at 138 K, phase I and phase II [Color figure can be viewed at wileyonlinelibrary.com]

phase I. The work by Ashcroft[97] established that the pressure within the range of 4 to 7 GPa was required for phase I to undergo the transition to phase II, whereas Parrinello's study[98] reported the stability of phase II over phase I in the region of 2–5 GPa based in the experimental work of Thiéry and Léger.[99] Recent work by Budzianowski[93] demonstrated that phase II of benzene was thermodynamically stable at pressures >0.91 GPa up to 5 GPa at 295 K. Their results clearly identified that the main structural change between phase I and phase II was the collapse of intermolecular voids, with all intermolecular distance becoming shorter by 0.2–0.3 Å shorter than those in phase I. As a result, the benzene molecules in phase II have closer contacts than those in phase I and experience stronger interactions between each other. Therefore, in the absence of the pressure and temperature effects phase II is more energetically stable than phase I. The scenario of $P$ = 0 GPa and $T$ = 0 K is considered in our calculations. Our estimations of the entropic changes associated with the transition of phase I to phase II indicate that at ambient pressure phase I may potentially convert to phase II at temperature below 95 K (for more detail see Table S16). Currently, the lowest temperature at which the crystal structure of phase I was recorded is 138 K, which may explain why it was never observed upon cooling down phase I.

In phase I, the benzene molecules are nearly perpendicular to each other, creating medium-sized voids in the crystal structure. Upon transitioning to phase II, such voids collapse, thus reducing the separation between benzene molecules (see Figure 11). As a result, these interact stronger than those in phase I, resulting in a larger lattice energy. This observation is further supported with increased number of C—C intermolecular distances in the close-contact range, below 6 Å, in phase II compared to those in phase I (see Figure 12). Therefore, it is not surprising that phase II has a stronger contribution from dispersion forces and a higher stability of the crystal structure overall.

Corrections for the higher level of theory in phase I were calculated to be 1.8 and 0.3 kJ·mol$^{-1}$ for two- and three-body effects, respectively (see Tables S7 and S8). These values were slightly higher in phase II with 3.8 kJ·mol$^{-1}$ for two body and 0.8 kJ·mol$^{-1}$ for three-body effects (see Tables S12 and S13). The counterpoise correction

for BSSE at the HF level was found to be 5.4 and 6.8 kJ·mol$^{-1}$ for phase I and phase II, respectively (see Tables S9, S10, S14, and S15). Including these corrections lead to the predicted lattice energies of −46.6 kJ·mol$^{-1}$ for phase I and −50.3 kJ·mol$^{-1}$ for phase II. As expected, phase II was found to be more thermodynamically stable by 3.7 kJ·mol$^{-1}$ as it was driven by stronger dispersion forces.

The crystal structure at 138 K was found to have the strongest lattice energy. This is not surprising considering that the other two structures were recorded at a higher temperature of 295 K. The differences in the stability of these crystal structures can be explained due to a subtle interplay of two- and three-body electrostatic and dispersion interactions. The proposed approach allows for the automatic extraction of these components during the calculation, thus giving an invaluable insight into the stability of each individual crystal structure.

## 4 | CONCLUSIONS

We have introduced a robust and inexpensive approach for the prediction of lattice energy of organic molecular crystals based on the combination of the FMO approach and the SRS-MP2 method. This approach chooses a reference molecule in the crystal structure and selects every single neighboring molecule present in the sphere of a particular radius, similar to the Harrison approach[72] used for the calculation of Madelung constant. Predicted lattice energies were shown to converge very fast already at a radius of 12 Å for the benzene crystal structure at 138 K as well as two other known polymorphs—phase I and phase II. Due to the nature of the FMO approach, lattice energies could be easily decomposed into two- and three-body components as well as electrostatic (HF) and dispersion (electron correlation) forces using the same calculation, thus allowing us to have an invaluable insight into the interplay of intermolecular forces on the stability of each crystal. Due to the inclusion of polarization effects for individual monomers, many-body effects beyond three-body are not necessary to be considered in the FMO framework. The benzene crystal structure at 138 K was found to have a lattice energy of −63.9 kJ·mol$^{-1}$. Inclusion of two corrections for a higher correlated level of theory and BSSE improved the value to −57.5 kJ·mol$^{-1}$, which is only within 1.6 kJ·mol$^{-1}$ of that calculated by Yang et al.[68] using a significantly more expensive approach requiring the calculation of four-body effects at CCSD(T). The stability of this crystal structure was attributed to two-body dispersion effects, with electrostatic forces playing a slightly destabilizing role.

The proposed approach was further assessed by predicting lattice energy of phase I and phase II polymorphs of benzene recorded at 295 K. The final lattice energies of were found to be −46.6 kJ·mol$^{-1}$ for phase I and −50.3 kJ·mol$^{-1}$ for phase II. Phase I was found to be less thermodynamically stable than phase II by 3.7 kJ·mol$^{-1}$. The differences in stability of these crystal structures could be explained due to the strength of dispersion forces in phase II, whose three-body contributions were found to be non-negligible. The proposed approach shows a significant promise not only in predicting lattice energies of organic crystals, but also in distinguishing between polymorphs. It gives the best prediction of lattice energy without the need for higher (and more expensive) correlated levels of theory and the development of specialized codes to perform FMO calculations.

## ACKNOWLEDGMENTS

The authors gratefully acknowledge a generous allocation of computer resources through the Monash *e*Research Centre, the National Computational Infrastructure and the Texas Advanced Computing Centre (TACC) at The University of Texas at Austin. This research was supported by the Australian Government through International PhD Scholarships for ALPN and TGM. The authors would like to thank Dr Dmitri Fedorov (AIST, Japan) for fruitful discussions.

## ORCID

*Anh L. P. Nguyen* https://orcid.org/0000-0001-9170-5468
*Thomas G. Mason* https://orcid.org/0000-0003-1131-6249
*Benny D. Freeman* https://orcid.org/0000-0003-2779-7788
*Ekaterina I. Izgorodina* https://orcid.org/0000-0002-2506-4890

## REFERENCES

[1] J. Haleblian, W. McCrone, *J. Pharm. Sci.* **1969**, *58*, 911.
[2] A. Llinàs, J. M. Goodman, *Drug Discovery Today* **2008**, *13*, 198.
[3] C.-H. Gu, H. Li, R. B. Gandhi, K. Raghavan, *Int. J. Pharm.* **2004**, *283*, 117.
[4] R. W. Lancaster, P. G. Karamertzanis, A. T. Hulme, D. A. Tocher, T. C. Lewis, S. L. Price, *J. Pharm. Sci.* **2007**, *96*, 3419.
[5] E. Lee, *Asian J. Pharm. Sci.* **2014**, *9*, 163.
[6] Guidance for Industry, ANDAs, *Pharmaceutical Solid Polymorphism*, US. Food and Drug Administration, Rockville, MD, USA **2007**.
[7] M. Neumann, M.-A. Perrin, *CrystEngComm* **2009**, *11*, 2475.
[8] A. J. Cabeza, G. M. Day, S. W. D. Motherwell, W. Jones, *Cryst. Growth Des.* **2007**, *7*, 100.
[9] A. Gavezzotti, G. Filippini, *J. Am. Chem. Soc.* **1995**, *117*, 12299.
[10] S. H. C. Chan, J. Kendrick, F. J. J. Leusen, *Angew. Chem., Int. Ed.* **2011**, *50*, 2979.
[11] A. J. C. Cabeza, G. M. Day, W. D. S. Motherwell, W. Jones, *Cryst. Growth Des.* **2006**, *6*, 1858.
[12] S. G. Stefan, J. Antony, S. Ehrlich, H. Krieg, *J. Chem. Phys.* **2010**, *132*, 154104.
[13] A. O. de la Roza, E. R. Johnson, *J. Chem. Phys.* **2012**, *137*, 054103.
[14] A. M. Reilly, A. Tkatchenko, *J. Phys. Chem. Lett.* **2013**, *4*, 1028.
[15] A. M. Reilly, A. Tkatchenko, *J. Chem. Phys.* **2013**, *139*, 024705.
[16] J. Moellmann, S. Grimme, *J. Phys. Chem. C* **2014**, *118*, 7615.
[17] A. M. Reilly, A. Tkatchenko, *Chem. Sci.* **2015**, *6*, 3289.
[18] A. Tkatchenko, M. Scheffler, *Phys. Rev. Lett.* **2008**, *102*, 073005.
[19] A. Tkatchenko, R. A. DiStasio Jr.., R. Car, M. Scheffler, *Phys. Rev. Lett.* **2012**, *108*, 236402.
[20] R. A. DiStasio, O. A. von Lilienfeld, A. Tkatchenko, *Proc. Natl. Acad. Sci.* **2012**, *109*, 14791.
[21] A. Ambrosetti, A. M. Reilly, D. S. RA Jr.., A. Tkatchenko, *J. Chem. Phys* **2014**, *140*, 18A508.
[22] J. Kendrick, F. J. J. Leusen, M. A. Neumann, J. van de Streek, *Chem. – Eur. J.* **2011**, *17*, 10736.
[23] A. M. Reilly, R. I. Cooper, C. S. Adjiman, S. Bhattacharya, A. D. Boese, J. G. Brandenburg, P. J. Bygrave, R. Bylsma, J. E. Campbell, R. Car, et al., *Acta Crystallogr., Sect. B: Struct. Sci.* **2016**, *72*, 439.
[24] C. Pisani, L. Maschio, S. Casassa, M. Halo, M. Schütz, D. Usvyat, *J. Comput. Chem.* **2008**, *29*, 2113.
[25] M. Marsman, A. Grüneis, J. Paier, G. Kresse, *J. Chem. Phys.* **2009**, *130*, 184103.

[26] A. Erba, C. Pisani, S. Casassa, L. Maschio, M. Schütz, D. Usvyat, *Phys. Rev. B* **2010**, *81*, 165108.
[27] L. Maschio, D. Usvyat, M. Schütz, B. Civalleri, *J. Chem. Phys.* **2010**, *132*, 134706.
[28] A. Grüneis, M. Marsman, G. Kresse, *J. Chem. Phys.* **2010**, *133*, 074107.
[29] L. Maschio, D. Usvyat, B. Civalleri, *CrystEngComm* **2010**, *12*, 2429.
[30] R. L. Jaffe, G. D. Smith, *J. Chem. Phys.* **1996**, *105*, 2780.
[31] P. Hobza, H. L. Selzle, E. W. Schlag, *J. Phys. Chem.* **1996**, *100*, 18790.
[32] S. Tsuzuki, T. Uchimaru, K. Matsumura, M. Mikami, K. Tanabe, *Chem. Phys. Lett.* **2000**, *319*, 547.
[33] S. Tsuzuki, H. P. Lüthi, *J. Chem. Phys.* **2001**, *114*, 3949.
[34] M. Ben, J. Hutter, J. VandeVondele, *J. Chem. Theory Comput.* **2012**, *8*, 4177.
[35] G. J. O. Beran, *Chem. Rev.* **2016**, *116*, 5567.
[36] H. Stoll, *Phys. Rev. B.* **1992**, *46*, 6700.
[37] H. Stoll, *J. Chem. Phys.* **1992**, *97*, 8449.
[38] H. Stoll, *Chem. Phys. Lett.* **1992**, *191*, 548.
[39] B. Paulus, *Phys. Rep.* **2006**, *428*, 1.
[40] G. J. Beran, *J. Chem. Phys.* **2009**, *130*, 164115.
[41] M. Kamiya, S. Hirata, M. Valiev, *J. Chem. Phys.* **2008**, *128*, 074103.
[42] G. J. Beran, S. Wen, K. Nanda, Y. Huang, Y. Heit, *Prediction and Calculation of Crystal Structures*, Vol. 345, Springer-Verlag, Berlin Heidelberg. Accurate and Robust Molecular Crystal Modeling Using Fragment-Based Electronic Structure Methods; **2014**.
[43] S. Hirata, M. Valiev, M. Dupuis, S. S. Xantheas, S. Sugiki, H. Sekino, *Mol. Phys.* **2005**, *103*, 2255.
[44] A. Hermann, P. Schwerdtfeger, *Phys. Rev. Lett.* **2008**, *101*, 183005.
[45] P. Schwerdtfeger, B. Assadollahzadeh, A. Hermann, *Phys. Rev. B* **2010**, *82*, 205111.
[46] O. Bludsky, M. Rubes, P. Soldan, *Phys. Rev. B: Condens. Matter Mater. Phys.* **2008**, *77*, 092103.
[47] S. Tsuzuki, H. Orita, K. Honda, M. Mikami, *J. Phys. Chem. B* **2010**, *114*, 6799.
[48] C. R. Taylor, P. J. Bygrave, J. N. Hart, N. L. Allan, F. R. Manby, *Phys. Chem. Chem. Phys.* **2012**, *14*, 7739.
[49] G. J. Beran, K. Nanda, *J. Phys. Chem. Lett.* **2010**, *1*, 3480 ISSN 1948-7185.
[50] S. Wen, G. J. Beran, *J. Chem. Theory Comput.* **2011**, *7*, 3733.
[51] S. Wen, G. J. Beran, *Cryst. Growth Des.* **2012**, *12*, 2169.
[52] S. Wen, G. J. Beran, *J. Chem. Theory Comput.* **2012**, *8*, 2698.
[53] K. Nanda, G. J. Beran, *J. Phys. Chem. Lett.* **2013**, *4*, 3165.
[54] O. Sode, S. Hirata, *J. Phys. Chem. A* **2010**, *114*, 8873.
[55] K. Gilliard, O. Sode, S. Hirata, *J. Chem. Phys.* **2014**, *140*, 174507.
[56] J. Li, O. Sode, S. Hirata, *J. Chem. Theory Comput.* **2014**, *11*, 224.
[57] K. Kazuo, I. Eiji, A. Toshio, N. Tatsuya, U. Masami, *Chem. Phys. Lett.* **1999**, *313*, 701.
[58] K. Nagayoshi, T. Ikeda, K. Kitaura, S. Nagase, *J. Theor. Ccomput. Chem.* **2003**, *02*, 233.
[59] D. G. Fedorov, K. Kitaura, *J. Phys. Chem. A* **2007**, *111*, 6904.
[60] P. J. Bygrave, N. L. Allan, F. R. Manby, *J. Chem. Phys.* **2012**, *137*, 164102.
[61] M. J. Gillan, D. Alfe, P. J. Bygrave, C. R. Taylor, F. R. Manby, *J. Chem. Phys.* **2013**, *139*, 114101 ISSN 0021-9606.
[62] M. J. Gillan, D. Alfe, F. R. Manby, *J. Chem. Phys.* **2015**, *143*, 102812 ISSN 0021-9606.
[63] J. Liu, L.-W. Qi, J. Z. H. Zhang, X. He, *J. Chem. Theory Comput.* **2017**, *13*, 2021 ISSN 1549-9618.
[64] J. Liu, X. He, *Phys. Chem. Chem. Phys.* **2020**, *22*, 12341.
[65] C. L. Brooks, *J. Solution Chem.* **1989**, *18*, 99.
[66] S. W. de Leeuw, J. W. Perram, E. R. S. ER, *A* **1980**, *373*, 27.
[67] P. P. Ewald, *Ann. Phys.* **1921**, *64*, 253.
[68] J. Yang, W. Hu, D. Usvyat, D. Matthews, M. Schütz, G. Chan, *Science* **2014**, *345*, 640.
[69] C. H. Borca, B. W. Bakr, L. A. Burns, D. C. Sherrill, *J. Chem. Phys.* **2019**, *151*, 144103.
[70] R. Sure, S. Grimme, *J. Comput. Chem.* **2013**, *34*, 1672.
[71] E. I. Izgorodina, U. L. Bernard, P. M. Dean, J. M. Pringle, D. R. MacFarlane, *Cryst. Growth Des.* **2009**, *9*, 4834 ISSN 1528-7483.
[72] W. A. Harrison, *Phys. Rev. B* **2006**, *73*, 212103.
[73] O. Emersleben, *Naturwissenschaften* **1959**, *46*, 64.
[74] S. Y. S. Tan, S. Acevedo, E. I. Izgorodina, *J. Chem. Phys.* **2017**, *146*, 064108.
[75] S. Y. S. Tan, L. Wylie, I. Begic, D. Tran, E. I. Izgorodina, *Phys. Chem. Chem. Phys.* **2017**, *19*, 28936.
[76] P. Jurečka, J. Šponer, J. Černý, P. Hobza, *Phys. Chem. Chem. Phys.* **2006**, *8*, 1985.
[77] J. Řezáč, K. E. Riley, P. Hobza, *J. Chem. Theory Comput.* **2011**, *7*, 2427.
[78] J. Rigby, E. I. Izgorodina, *J. Chem. Theory Comput.* **2014**, *10*, 3111.
[79] J. Rigby, S. B. Acevedo, E. I. Izgorodina, *J. Chem. Theory Comput.* **2015**, *11*, 3610.
[80] T. P. Tauer, C. D. Sherrill, *J. Phys. Chem. A* **2005**, *109*, 10475.
[81] M. R. Kennedy, A. R. McDonald, A. E. DePrince, M. S. Marshall, R. Podeszwa, C. D. Sherrill, *J. Chem. Phys.* **2014**, *140*, 121104.
[82] T. Nakano, T. Kaminuma, T. Sato, Y. Akiyama, M. Uebayasi, K. Kitaura, *Chem. Phys. Lett.* **2000**, *318*, 614.
[83] T. Nakano, T. Kaminuma, T. Sato, K. Fukuzawa, Y. Akiyama, M. Uebayasi, K. Kitaura, *Chem. Phys. Lett.* **2002**, *351*, 475.
[84] M. S. Gordon, D. G. Fedorov, S. R. Pruitt, L. V. Slipchenko, *Chem. Rev.* **2012**, *112*, 632.
[85] D. G. Fedorov, R. M. Olson, K. Kitaura, M. S. Gordon, S. Koseki, *J. Comput. Chem.* **2004**, *25*, 872.
[86] D. G. Fedorov, K. Kitaura, *J. Chem. Phys.* **2004**, *121*, 2483.
[87] D. G. Fedorov, K. Kitaura, *J. Chem. Phys.* **2004**, *120*, 6832.
[88] D. G. Fedorov, K. Kitaura, *Chem. Phys. Lett.* **2006**, *433*, 182.
[89] D. G. Fedorov, K. Ishimura, T. Ishida, K. Kitaura, P. Pulay, S. Nagase, *J. Comput. Chem.* **2007**, *28*, 1476.
[90] D. G. Fedorov, K. Kitaura, *J. Comput. Chem.* **2007**, *28*, 222.
[91] P. Halat, Z. L. Seeger, S. Acevedo, E. I. Izgorodina, *J. Phys. Chem. B* **2017**, *121*, 577.
[92] G. E. Bacon, N. A. Curry, S. A. Wilson, R. Spence, Proc. R. Soc. London A. **1964**, *279*, 98.
[93] A. Katrusiak, M. Podsiadło, A. Budzianowski, *Cryst. Growth Des.* **2010**, *10*, 3461.
[94] M. W. Schmidt, K. K. Baldridge, J. A. Boatz, S. T. Elbert, M. S. Gordon, J. H. Jensen, S. Koseki, N. Matsunaga, K. A. Nguyen, S. Su, T. L. Windus, M. Dupuis, J. A. Montgomery, *J. Comput. Chem.* **1993**, *14*, 1347.
[95] S. F. Boys, F. Bernardi, *Mol. Phys.* **1970**, *19*, 553.
[96] R. M. Parrish, L. A. Burns, D. G. A. Smith, A. C. Simmonett, A. E. DePrince, E. G. Hohenstein, U. Bozkaya, A. Y. Sokolov, R. D. Remigio, R. M. Richard, et al., *J. Chem. Theory Comput.* **2017**, *13*, 3185.
[97] X.-D. Wen, R. Hoffmann, N. W. Ashcroft, *J. Am. Chem. Soc.* **2011**, *133*, 9023.
[98] P. Raiteri, R. Martoňák, M. Parrinello, *Angew. Chem., Int. Ed.* **2005**, *44*, 3769.
[99] M. M. Thiéry, J. M. Léger, *J. Chem. Phys.* **1988**, *89*, 4255.

## SUPPORTING INFORMATION

Additional supporting information may be found online in the Supporting Information section at the end of this article.

**How to cite this article:** Nguyen ALP, Mason TG, Freeman BD, Izgorodina EI. Prediction of lattice energy of benzene crystals: A robust theoretical approach. *J Comput Chem*. 2020;1–13. https://doi.org/10.1002/jcc.26452